

Safety study on HIC containing waste resin with respect to hydrogen release

Shuai-Wei Zhao¹ · Mei-Lan Jia¹ · Xing-Qian Jiao² · Meng-Qi Qiu² · Hong-Hui Li¹ · Yu-Chen Liu¹ · Liang Mao¹ · Wei Liu¹ · Dong Liang¹

Received: 20 December 2017 / Revised: 18 May 2018 / Accepted: 1 October 2018 / Published online: 13 March 2019
© China Science Publishing & Media Ltd. (Science Press), Shanghai Institute of Applied Physics, the Chinese Academy of Sciences, Chinese Nuclear Society and Springer Nature Singapore Pte Ltd. 2019

Abstract To explore the behavior of radiolytically produced hydrogen release from the waste resin stored in a high integrated container (HIC), and the mechanism of hydrogen diffusion in a near-surface disposal facility, both experimental studies and numerical simulations were performed through an accelerated irradiation test and simulated disposal, respectively. Results indicated that, 100 years after disposal, the highest hydrogen concentration appeared in the cell where the HICs were placed. The volume fraction for different scenarios postulated in the numerical simulation was 2.64% for Scenario 1, 2.28% for Scenario 2, and 3.965% for Scenario 3, all of which are lower than the hydrogen explosion limit of 4.1%. The results indicated that the simulated HIC disposal scheme is safe.

Keywords Radioactive waste resin · High integrated container · Repository · Radiolysis · Hydrogen release

1 Introduction

To reduce the volume of waste stored in a near-surface repository, the high density polyethylene-high integrated containers (referred to as HIC) are used, instead of cement solidification, at some nuclear power plants (NPPs) in

China to contain radioactive waste resins for direct disposal. For the accumulation of dose from radionuclides adsorbed on waste resin, these resins are subjected to ionizing irradiation by radionuclides trapped in their structures or stored nearby, thereby resulting in their decomposition and an increased risk of the flammable gas generated in the HIC and accumulated in repository during storage and disposal periods. As Cs-137/Cs-134/Co-60 is the primary radioactive nuclides absorbed on resins, the gamma-induced decomposition of ion exchange materials is the primary source. The radionuclides adsorbed on waste resin could cause the radiolysis of the resin, simultaneously generating radiolytic gases, including hydrogen gas.

Few studies have focused on hydrogen release from the waste resin stored in HICs, the mechanism of hydrogen diffusion in a near-surface disposal facility, and their effects on disposal safety. Many attempts to explain such a radiation damage by proposing degradation mechanisms have been reported [1–7]. Swyler [1] demonstrated that the gamma irradiation of these resins in OH- and Cl-form produced molecular hydrogen with relatively high radiation yields and trimethylamine gas in lower proportions. Hall and Streat [5] revealed that primary, secondary, and tertiary amines and ammonia were the primary aqueous decomposition products released when these resins were irradiated in the presence of water. Traboulsi [7] reported the gamma radiation effect mechanism on gas production in anion exchange resins, where hydrogen was produced primarily by the degradation of the ammonium functional groups and the radiolysis products, in particular the amines. Baidak and Laverne [8] reported that enhanced hydrogen production was observed with high water content, and that the radiolytic decomposition of the compounds released

✉ Hong-Hui Li
yz2021hh@163.com

¹ China Institute for Radiation Protection, Taiyuan 030006, China

² Sichuan Environmental Protection and Engineering CO., LTD., CNNC, Guangyuan 610006, China

during irradiation in the aqueous phase contributed primarily to the generation of molecular hydrogen.

Initially, the HIC containing wet waste resin was sent to a solid waste storage facility at the NPPs in China for temporary storage, while waiting for the final disposal at a repository. During the temporary storage at the NPPs, because an installed ventilation system can timely discharge the combustible gases released from the waste resin contained in the HIC, hydrogen explosion owing to the accumulation of combustible gases will not occur. However, a ventilation system is not installed in the disposal facility in the present study. When the hydrogen concentration exceeds its explosion limit, an explosion might occur. Therefore, both experimental studies and theoretical calculations must focus on the release and diffusion of hydrogen to assess their effects on the disposal safety.

2 Disposal plan

A conceptual scheme was designed for integrating the HICs containing waste resins and the cemented waste packages into a near-surface repository. The floor and surrounding walls of the repository were built with a reinforced-concrete structure and the repository roof was of a cast-in-place reinforced-concrete structure. A V-shaped roof is covered with clay, with the middle being thicker than its two swings. Figure 1 shows a schematic diagram of the near-surface repository.

Four-row monolayer square cells were set on the bottom of the disposal units, as shown in Fig. 2, for the disposal of the HICs. Both the roof and wall were composed of 300-mm thick concrete, with each square cell containing an HIC. A gap existed between the HIC and cell inner wall. Two layers of 400-L waste packages were placed around the cell, with a 100-mm-thick cement mortar layer paved between them. After constructing according to the

description above, both the HIC and two layers of 400-L waste packages were casted integrally with cement mortar, to ensure a 100-mm thickness at the upper cover of the 400-L waste packages. Further, 200-L waste packages were stacked at the third layer and 400-L waste packages at the fourth to the seventh layers. Subsequently, all gaps existing between the waste packages were filled with a 100-mm-thick cement mortar.

3 Experimental study on hydrogen release

3.1 General concept

The purpose of the experimental study on the hydrogen release from resin is to determine the hydrogen release rate from the waste resin stored in the HIC, analyze the gas composition released from waste resin radiolysis, and provide input source terms to the present study on hydrogen diffusion in a disposal facility.

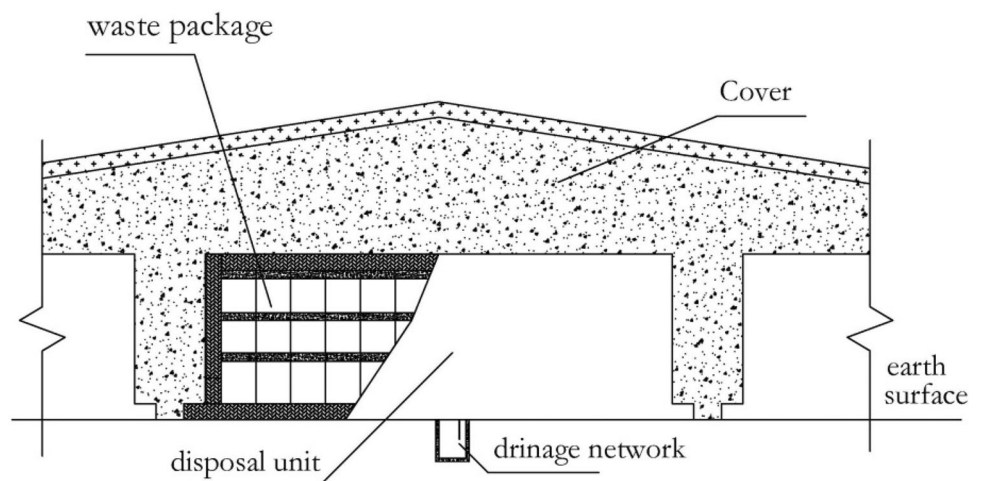
To complete this study, a series of studies have been performed on irradiated container design, small batch production and sealing test, resin purchase and pretreatment, design and confirmation of sample irradiation plan, and measurement and analysis of the amount and components of gases in an irradiated sample. The specific process of this study is shown in Fig. 3.

3.2 Experimental materials and irradiated containers

3.2.1 Experimental resin

The experimental resin used in the present study was fresh resin, with the same model number as that stored in the HIC, as shown in Table 1.

Fig. 1 Schematic diagram of the ground-surface repository



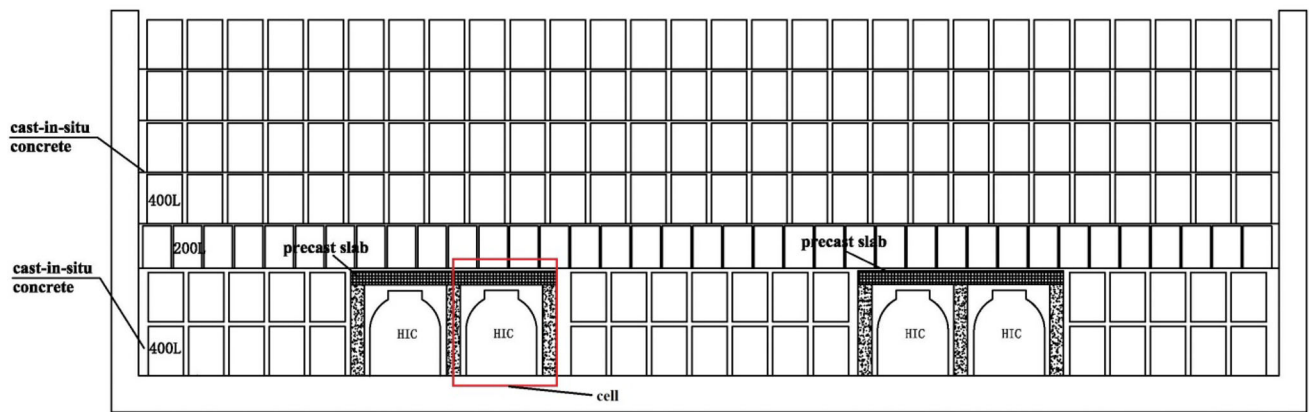
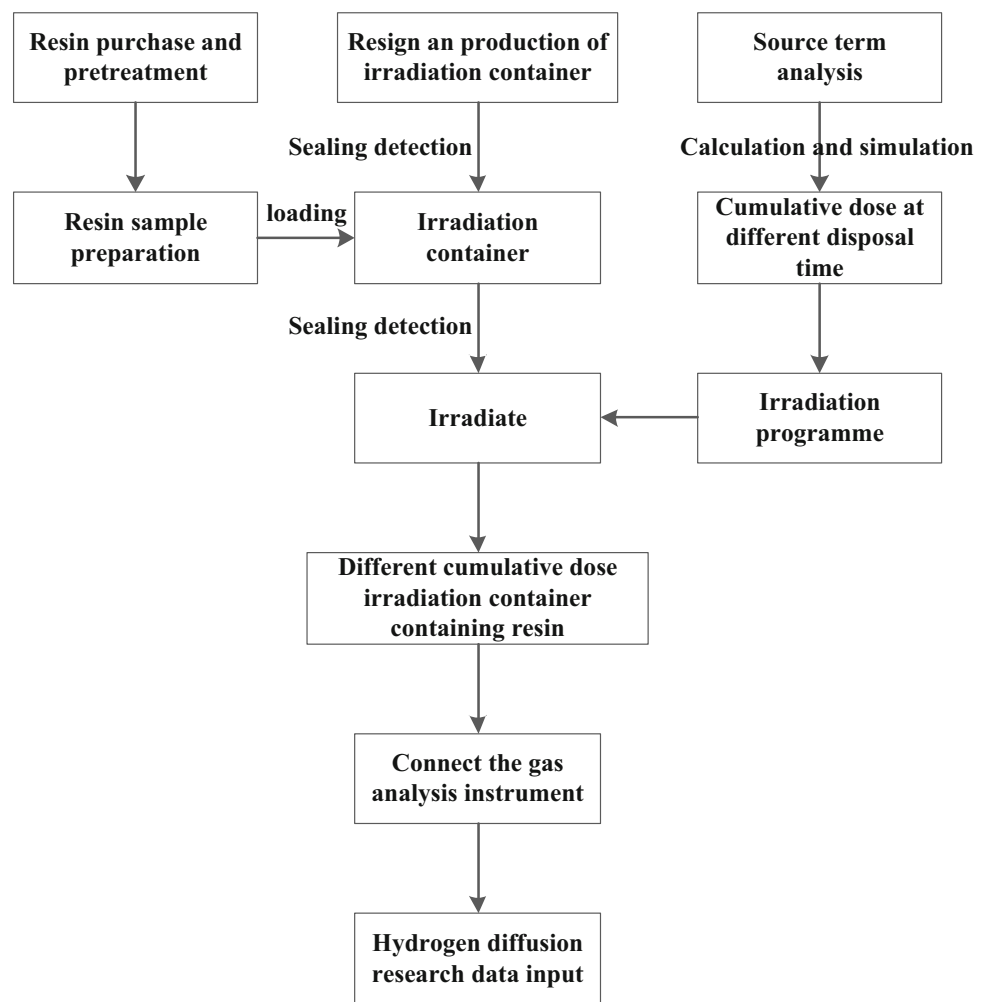


Fig. 2 Schematic diagram of HICs in disposal unit at near-surface repository

Fig. 3 Flow chart of the experimental study



3.2.2 Irradiation container

An irradiated container is intended to load the experimental resin with the concept of the containment of radiolytic gas generated during the accelerated irradiation. Therefore, the irradiated containers must satisfy the

requirements of leakproofness, pressure-resistance, and radiation resistance, and be able to connect to a gas analytical instrument for the easy discharge of radiolytic gas after irradiation.

The irradiated container (see Fig. 4a) is made of a molded stainless steel pipe and plate (at top and bottom)

welded together. At the top of each container, an ϕ 12-mm 1/2VCR interface was designed for resin filling and connected to the other 1/2VCR interface via a full metal bellow seal valve (see Fig. 4b), and compacted with the sealing gasket. A container of height 300 mm, thickness 2 mm, and diameter 62 mm was used. The effective volume was 0.9 L, with a bearing pressure of 1.5 MPa. A leak-check test was conducted after the completion of manufacture to ensure the container tightness and the maximum pressure-bearing of 1.5 MPa.

3.3 Accumulated irradiation dose in experiment

The activity concentrations of the primary radionuclides adsorbed on the waste resin are shown in Table 2. The radioactivity constants of those nuclides are shown in Table 3. The timescale of the study is 300 years, approximately 10 times the maximum half-life of those in the source terms.

The upper limit of the accumulated absorbed dose to the resin are available through calculations for the time periods of 1, 5, 10, 30, 60, 100, and 300 years after repository closure, as shown in Table 4.

3.4 Resin filling and irradiation

The cation and anion resins were soaked separately in the test barrel for 7 days while awaiting water saturation, and were subsequently dewatered to ensure no free water existed in them. The dewatered cation and anion resins were filled into the irradiated containers in terms of a volume ratio of 1:1 while awaiting transportation to the irradiation company after a qualified leakage check. The weight of cation and anion resins filled into irradiated containers and the filling fraction of resins in irradiated containers can be seen in Table 5.

The irradiation and dose control process were undertaken by China Isotope & Radiation Corporation, using the BFT-IV Cobalt 60 irradiation device equipped with a 600,000 Ci Cobalt 60 single-plate source.

3.5 Measurement and data processing

The pressure inside the irradiated container was tested first after irradiation; subsequently, the gas compositions

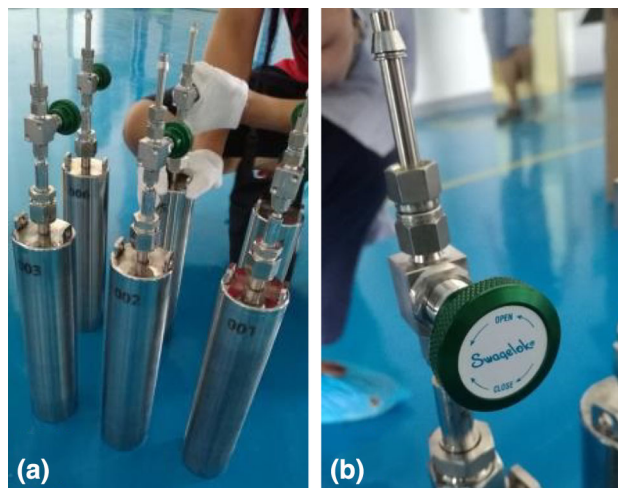


Fig. 4 Photographs of irradiated container (a) and full metal bellow seal valve (b)

Table 2 Activity concentration of radionuclides adsorbed on waste resin

Nuclide	Activity concentration (GBq/m ³)
Cs-134	2.39E+03
Cs-137	3.34E+03
Co-60	8.95E+01
Total	5.82E+03

Table 3 Radioactivity constants of nuclides

Nuclide	Half-life (y)	Air kerma-rate constant (Γ_k)
Cs-134	5.27E+00	5.72E−17
Cs-137	3.00E+01	2.12E−17
Co-60	2.06E+00	8.67E−17

therein were analyzed using gas chromatography, as shown in Table 6.

The pressure measurement for the irradiated container indicated that the pressure inside the three irradiated containers exposed to an accumulated dose of 56,100 Gy (1 year after disposal) was negative, as shown in Table 6. The irradiation test was conducted at a high dose rate, and resulted in a short time period to such an accumulated dose

Table 1 Characteristics of experimental resin

Type	Model	Wet apparent density (g/mL)	Wet true density (g/mL)	Water content (%)
Cation exchange	GR-2-0 NG	0.82	1.22	48.3
Anion exchange	GR-1-9 NG	0.70	1.08	58.6

Table 4 Upper limits of accumulated absorbed dose to resin at different time periods after disposal

Post-disposal time (y)	Upper limit of accumulated absorbed dose (Gy)	Post-disposal time (y)	Upper limit of accumulated absorbed dose (Gy)
1	56,100	60	751,500
5	201,000	100	949,500
10	310,500	300	1,041,000
30	583,200		

Table 5 Weight of cation and anion resins filled into irradiated containers and filling fraction

Serial number of sample group	Upper limit of accumulated dose (Gy)	Time period (y)	Cation resin (kg)	Anion resin (kg)	Filling fraction (%)
1	56,100	1	0.2162	0.1910	60
2	201,000	5	0.2162	0.1910	60
3	310,500	10	0.2162	0.1910	60
4	583,200	30	0.1892	0.1671	53
5	751,500	60	0.1892	0.1671	53
6	949,500	100	0.1892	0.1671	53
7	1,041,000	300	0.1892	0.1671	53

Three parallel samples were set for each sample group, with a total of 21 irradiated containers loaded with resin

that could be reached during a 1-year period under the actual disposal conditions. The test resin reacted rapidly with oxygen in the container at a high dose rate, leading to the consumption of a large amount of oxygen, but without enough radiolytic gas to generate in the short irradiation time period. Thus, the gas consumption inside the irradiated container is greater than the gas generation. This may be the reason for the negative pressure inside the container. The mechanism of resin radiolysis is too complicated to interpret, and requires further study.

Based on the gas state equation, the ambient temperature on the day of resin loading test, the ambient temperature on the day of measuring the pressure in the irradiated container after irradiation, along with the corresponding container pressure and the inventory of radiolytic gas at different accumulated doses (ignoring the change in atmospheric pressure), the average release rate of the radiolytic gas from the mixed resins per unit mass per year in different disposal time periods (0–1, 1–5, 5–10, 10–30, 30–60, 60–100, and 100–300 years) are estimated, as shown in Table 7.

The estimated result of hydrogen release rate is modified using the diffusion coefficient of hydrogen in stainless steel, based on the amount of radiolytic gas released from the mixed resin per unit mass and their fraction in the radiolytic gas, together with considering the potential penetration of hydrogen in the irradiated container through outside the stainless steel wall through diffusion. The mechanism of hydrogen diffusion varies considerably depending on the internal steel structure. For example, the hydrogen diffusion coefficient for different steels ranges from 10^{-9} to 10^{-20} m²/s [9]. The diffusion coefficient of hydrogen through Model 304 stainless steel is 9.26×10^{-12} m²/s [10], which was measured using the electrochemical permeation method. The hydrogen loss owing to permeation was calculated according to both the start and end times of the irradiation test on each irradiated container containing mixed resins and the measurement time of radiolytic gas in each irradiated container. The average release rate of hydrogen from the mixed resins per unit mass during different disposal time periods (0–1, 1–5, 5–10, 10–30, 30–60, 60–100, and 100–300 years) are shown in Table 7.

4 Simulation of hydrogen release and diffusion in repository

4.1 Physical model of hydrogen mass transfer (HMT) in repository

Based on the disposal scheme, a disposal unit contains four disposal cells each with one HIC, stacked with cement-solidified waste packages in the surrounding and on the top of each cell. The gap is filled with cement mortar between the waste packages and/or between the waste package and disposal cell. The floor and surrounding wall of the repository are of reinforced-concrete structure, and the repository roof is a cast-in-place reinforced-concrete structure covered with clay, called the analytical unit of the HMT. As shown in Figs. 1 and 2, the four disposal cells are symmetrically distributed. For modeling, half of the disposal unit was regarded as an analytical unit.

Table 8 illustrates three HMT scenarios within a disposal unit considered in this study based on the analytical time scale of 300 years, waste package lifetime of 10 to 140 years [11], and additional hydrogen release from cemented waste resin.

The simplified equivalent two-dimensional models for three HMT scenarios are illustrated in Fig. 5.

Table 6 Pressure in irradiated container and average value of radiolytic gas composition at different accumulated doses

Serial number of sample group	Accumulated dose (Gy)	Relative pressure(Pa)	Absolute pressure (Pa)	H ₂	CH ₄	Other hydrocarbons	Incombustible gas
1	56,100	– 1E3	1.00E+05	29.63	0.02	0.00	70.35
2	201,000	2.16E4	1.23E+05	52.12	0.14	0.01	47.73
3	310,500	3.20E4	1.33E+05	54.30	0.24	0.17	45.29
4	583,200	5.00E4	1.56E+05	54.60	0.27	0.03	45.09
5	751,500	2.08E5	3.09E+05	68.25	0.26	0.01	31.48
6	949,500	4.53E5	5.54E+05	65.73	0.42	0.01	33.84
7	1,041,000	5.68E5	6.69E+05	62.45	0.26	0.01	37.28

Table 7 Average release rate of radiolytic gas

Average release rate of radiolytic gas from mixed resins per unit mass (mol/kg/y)	Average release rate of hydrogen from mixed resins per unit mass (mol/kg/y)	Time period (y)
1.13E–02	3.35E–03	0–1
3.00E–03	1.56E–03	1–5
1.10E–03	6.00E–04	5–10
1.10E–03	6.01E–04	10–30
3.35E–03	2.29E–03	30–60
4.03E–03	2.65E–03	60–100
3.78E–04	2.36E–04	100–300

4.2 Mathematical model of HMT in disposal unit

4.2.1 Hydrogen release from HIC

Owing to irradiation, the hydrogen generated in the waste resin stored in the HIC diffuses into the HIC head and subsequently into the disposal unit through the vent on the top of the HIC head. Assuming that the radiolytic gas (hydrogen) in the HIC is distributed homogeneously, the diffusion coefficient of hydrogen through the vent is 1.5×10^{-5} mol/s at 25 °C. Hydrogen is released at a rate greater than that at which it was generated in the normal condition. Consequently, the bottleneck effect does not occur during hydrogen release from the HIC. The amount of hydrogen released from the HIC varies with time, as expressed by Eq. (1):

$$\frac{dN(\text{gas}, t)}{dt} = V \cdot N(\text{gas}, t) - 5 \cdot R \cdot \Delta x, \tag{1}$$

where $N(\text{gas}, t)$ is the average release rate of hydrogen from the mixed resins per unit mass, as shown in Table 7, R is the diffusion coefficient of hydrogen through the vent, V represents the effective volume of the HIC with a value

of 2.86 m^3 , and Δx is the mole fraction of gas at both sides of the vent.

4.2.2 Diffusion of hydrogen in disposal unit

The hydrogen generation in waste resins is affected by the activity concentration of radionuclides adsorbed on them, and exhibits variation with time. The migration of hydrogen in the disposal unit is also a transient process varying with time. The HMT consists of four mass transfer phases:

- (1) Hydrogen generated in the HIC can be all vented through the filter and will not accumulate in the HIC; that is to say, all of the hydrogen generated in the HIC enters the cell in the disposal unit. Thus, Eq. (1) can be simplified to Eq. (2):

$$\bar{N}_F = V \cdot N(\text{gas}, t) = 5 \cdot R \cdot \Delta x, \tag{2}$$

where \bar{N}_F represents the amount of hydrogen discharged through a single HIC, mol/s.

- (2) Hydrogen diffused into disposal unit cell through the HIC filter can be described by Eq. (3):

$$\frac{\partial c_H^B}{\partial t} = D_1 \frac{\partial}{\partial x} \left(\frac{\partial c_H^B}{\partial x} \right) + D_1 \frac{\partial}{\partial y} \left(\frac{\partial c_H^B}{\partial y} \right), \tag{3}$$

where c_H^B represents the mole concentration of hydrogen in the cell, mol/m³; D_1 is the diffusion coefficient of hydrogen in the gas phase, m²/s.

- (3) Diffusion of hydrogen in a filled cement mortar can be described by Eq. (4):

$$\varepsilon_d \frac{\partial c_H^d}{\partial t} = D_2 \frac{\partial}{\partial x} \left(\frac{\partial c_H^d}{\partial x} \right) + D_2 \frac{\partial}{\partial y} \left(\frac{\partial c_H^d}{\partial y} \right), \tag{4}$$

where c_H^d represents the mole concentration of hydrogen in cement mortar between the waste packages, mol/m³; D_2 is the effective HDC in cement mortar, m²/s; ε_d is the porosity in concrete or cement mortar.

Table 8 Modeled mass transfer scenarios

Number	HMT process
Scenario 1	Radiolytic gas (hydrogen) generated in the HIC is diffused first into the cell and subsequently, through the cell concrete wall, to the cement mortar gap, followed by to the cover layer (compacted clay), and finally spreading to the outer environment. It is assumed that the waste package is not corroded, and the gas does not diffuse through the waste package or cement solidified waste, but only diffuse through the cement mortar between the waste packages
Scenario 2	Radiolytic gas (hydrogen) generated in the HIC is first diffused into the cell and subsequently diffused through the concrete wall of the cell to the cement mortar gap and the cement solidified waste, followed by into the cover layer (compacted clay), and eventually spreading into the environment. Assuming that the waste packages is corroded completely, the gas can diffuse through the waste package or cement solidified waste, and the cement mortar between the waste packages
Scenario 3	Radiolytic gas (hydrogen) generated in the HIC is diffused first into the cell and subsequently through the concrete wall of the cell, into the cement mortar gap and the cement solidified waste, followed by into the cover layer (compacted clay), and finally spreading to the outer environment. Assuming that the waste package is corroded completely, the gas can diffuse through the waste package, cement solidified waste, and cement mortar between the waste packages, with consideration of the diffusion of hydrogen generated in the waste resin confined in the cement solidified waste in the disposal unit

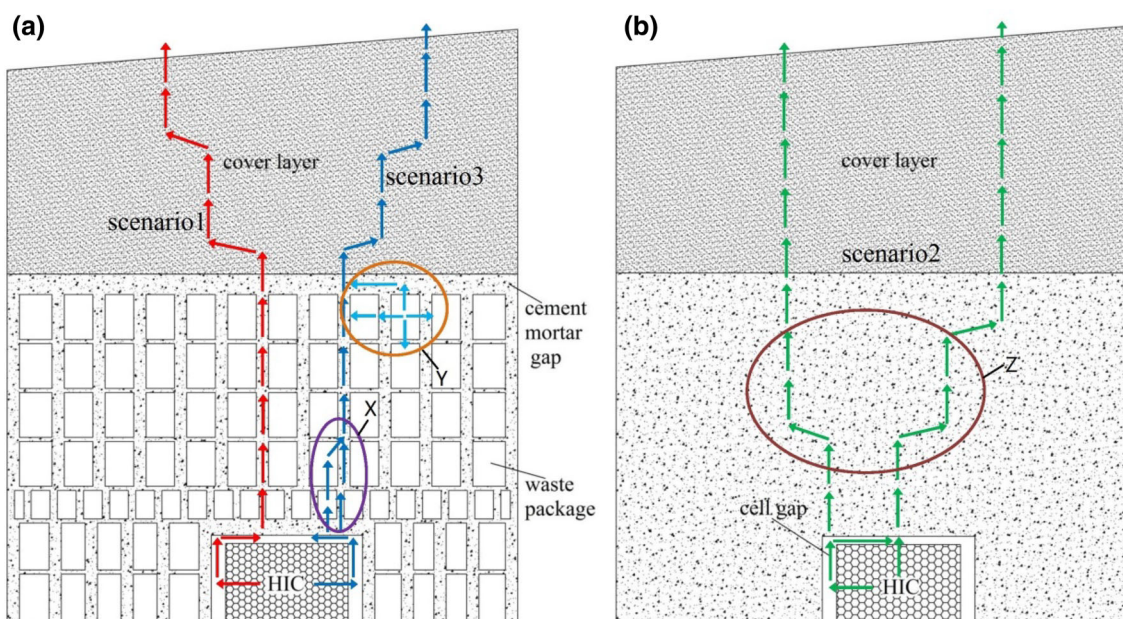


Fig. 5 Simplified equivalent two-dimensional models for HMT Scenario 1, Scenario 3 (a) and Scenario 2 (b). X—hydrogen diffuse through waste packages (corrosion); Y—diffusion of hydrogen

generated in waste resin confined in cement solidified waste; Z—hydrogen can diffuse into cement mortar gap and cement solidified waste

Equation (4) is applicable to Scenarios 1 and 2, where concrete and cement mortar are involved, but without considering the hydrogen release from the waste resin being solidified. In Scenario 3, it is also necessary to consider the hydrogen release from the waste resin being solidified; therefore, Eq. (4) becomes Eq. (5):

$$\varepsilon_d \frac{\partial c_H^d}{\partial t} = D_2 \frac{\partial}{\partial x} \left(\frac{\partial c_H^d}{\partial x} \right) + D_2 \frac{\partial}{\partial y} \left(\frac{\partial c_H^d}{\partial y} \right) + \eta \cdot N(\text{gas}, t), \tag{5}$$

where η represents the amount of resin cemented in the waste package. It is assumed in this study that the waste resin packages in a disposal unit constitutes 13% of the

total waste packages in volume, with each containing 35% waste resin in volume.

4.2.3 Diffusion of hydrogen in cover

The migration of hydrogen in the cover (compacted clay layer) is influenced by the effect of diffusion and adsorption, as described in Eq. (6):

$$\varepsilon_r \frac{\partial c_H^f}{\partial t} = D_3 \frac{\partial}{\partial x} \left(\frac{\partial c_H^f}{\partial x} \right) + D_3 \frac{\partial}{\partial y} \left(\frac{\partial c_H^f}{\partial y} \right) - S, \tag{6}$$

where c_H^f represents the mole concentration of hydrogen in the compacted clay layer, mol/m^3 ; D_3 is the effective HDC

in the compacted clay layer, m^2/s ; ε_f is the porosity of the compacted clay; S is the adsorption of hydrogen on clay.

Considering the adsorption of hydrogen on clay as a physical process in the disposal condition, the radiolytic gas can occupy the adsorption sites on clay, and the adsorbed amount of hydrogen can only occupy a small fraction of the total on clay. Thus, the adsorption of hydrogen on clay is negligible in calculations. Equation (6) can be simplified to Eq. (7):

$$\varepsilon_f \frac{\partial c_H^f}{\partial t} = D_3 \frac{\partial}{\partial x} \left(\frac{\partial c_H^f}{\partial x} \right) + D_3 \frac{\partial}{\partial y} \left(\frac{\partial c_H^f}{\partial y} \right). \quad (7)$$

After obtaining the necessary parameters, of which the most important is the diffusion coefficient of hydrogen in different media, the hydrogen concentration varying in time in the repository can be obtained through solving the equations mentioned above.

4.3 Diffusion parameters of hydrogen

Based on the disposal scheme, the diffusion parameters of hydrogen in the disposal unit include the following:

- (1) Intrinsic diffusion coefficient of hydrogen
The HDC (D_1) in the atmosphere ranges from 0.6×10^{-4} to $0.8 \times 10^{-4} m^2/s$ at room temperature [12], using $0.8 \times 10^{-4} m^2/s$ for a conservative calculation.
- (2) HDC in porous material

Concrete, cement mortar, and compacted clay are porous heterogeneous materials, with complicated distributions of the internal pore and large numbers of interconnecting holes and blind holes. With wide varieties of pore size distribution, the diffusion of hydrogen in porous materials includes the Knudsen diffusion and surface diffusion in addition to the intrinsic diffusion in larger pores. The effective HDC is a more appropriate parameter to describe the diffusion of hydrogen in porous materials.

The diffusion of hydrogen in porous materials is affected by both the dynamic characteristics of hydrogen and the form of the porous material. Two primary factors influence hydrogen diffusion in concrete. First, the higher water-to-cement ratio in concrete will lead to a higher porosity of concrete and subsequently a higher HDC. In contrast, the HDC is generally lower for a higher quality of concrete with a higher compactibility. Next, a greater relative humidity might lead to a smaller HDC in concrete. On the contrary, when the water content in concrete is lower or the concrete is drier, the diffusion of hydrogen in concrete is faster. In addition, the HDC in concrete becomes higher with the increasing temperature at the repository.

When the degree of water saturation at the repository is not high, when the water-to-cement ratio is 0.56, the effective

HDC is $2.1 \times 10^{-6} m^2/s$ for concrete and also approximates to the same value for cement mortar [13–17]. Therefore, the benchmark value of the effective HDC (D_2) in concrete materials was $2.1 \times 10^{-6} m^2/s$ for model calculation in the present study. The effective porosity (ε_d) of the concrete materials was 0.2 for a conservative computation.

For the clay materials with similar physicochemical properties to compacted clay, the cover consists of an HDC ranging from 1×10^{-7} to $2 \times 10^{-7} m^2/s$ at room temperature [18–20]. For a conservative calculation, the HDC (D_3) in compacted clay was $1 \times 10^{-7} m^2/s$ and the porosity of the compacted clay (ε_f) was 0.15.

4.4 Computed result of HMT

The physical and mathematic models for the HMT in the repository were solved and analyzed using the COMSOL Multiphysics numerical simulation software. The three scenarios demonstrated the similar characteristics of hydrogen distribution at the repository at different times. The hydrogen concentration in the surrounding area of the cell is higher than that in any other locations at the repository. The closer to the margin of the repository, the lower is the hydrogen concentration. The hydrogen concentration at the bottom of the repository is higher than that at the top because the hydrogen diffusion occurs beyond the repository. The highest concentration appears around the cell. Within the cell, the hydrogen shows a fast increase in the cell during the first 100 years after repository closure and subsequently a downward trend after 100 years.

Some differences exist between Scenarios 2 and 1. Waste package damage could lead to increased hydrogen migration channels and storage pores in the disposal unit in Scenario 2, thus allowing for hydrogen to not only migrate along the gap between the waste packages filled with cement mortar, but also to transfer through the cement solidified waste. This facilitates the migration and release of hydrogen from the disposal unit. Compared to Scenario 2, because the waste resin solidified in the cement solidified waste can release hydrogen in Scenario 3, the hydrogen release source items in the model calculation will be increased. The highest hydrogen concentration in the cell of the disposal unit, based on simulations, is 1.18 mol/m^3 in Scenario 1, 1.02 mol/m^3 in Scenario 2, and 1.77 mol/m^3 in Scenario 3. The hydrogen volume fraction in the three scenarios in descending order is Scenario 3 (3.965%), Scenario 1 (2.64%), and Scenario 2 (2.28%). The calculated concentrations of hydrogen for these three scenarios (released into ambient atmosphere through compacted clay) are of the order of 10^{-5} mol/m^3 . It was found that Scenario 3 is the most conservative in the simulation study, in which the highest concentration of hydrogen in the cell of the disposal unit is below the explosion limit of hydrogen.

5 Conclusion

Three physical scenarios concerning hydrogen diffusion and migration were established based on the repository disposal scheme. The following conclusions are drawn through model calculation and data analysis:

- (1) In general, no significant difference was found between the three scenarios in the concentration distribution of hydrogen with time. The hydrogen concentration at the bottom of the repository was higher than that at the top because the hydrogen diffusion occurred beyond the repository. For Scenarios 1 and 2, the hydrogen concentration around the cell was higher than in any other locations at the repository. The closer to the margin of the repository, the lower is the hydrogen concentration. However, for Scenario 3, this variation trend is not obvious because of the hydrogen release from the cement solidified waste.
- (2) The highest hydrogen concentration was calculated in terms of conservative parameters for three scenarios in the disposal unit, appears all in the cell. They were 1.18 mol/m³ in Scenario 1, 1.02 mol/m³ in Scenario 2, and 1.77 mol/m³ in Scenario 3. The hydrogen volume fractions in the three scenarios in descending order were Scenario 3 (3.965%), Scenario 1 (2.64%), and Scenario 2 (2.28%), all of which were below the hydrogen explosion limit (4.1%).
- (3) The highest hydrogen concentration in the cover surface of the repository was in the order of 10⁻⁵ mol/m³, which was significantly below the explosion limit of hydrogen.
- (4) The release from the HIC of hydrogen generated by the radiolysis of waste resin stored in the HIC did not affect the safety of the repository.

References

1. K.J. Swyler, C.J. Dodge, R. Dayal, Irradiation effects on the storage and disposal of radwaste containing organic ion-exchange media. Report NUREG/CR-3383: United States Nuclear Regulatory Commission (1983). <https://doi.org/10.2172/5088342>
2. O. Debré, B. Nsouli, J.P. Thomas et al., Irradiation-induced modifications of polymers found in nuclear waste embedding processes Part II: the ion-exchange resin. *Nucl. Instrum. Methods B* **131**, 321–328 (1997). [https://doi.org/10.1016/s0168-583x\(97\)00337-6](https://doi.org/10.1016/s0168-583x(97)00337-6)
3. A. Traboulsi, N. Dupuy, C. Rebufa et al., Investigation of gamma radiation effect on the anion exchange resin Amberlite IRA-400 in hydroxide form by FTIR and ¹³C NMR spectroscopy. *Anal. Chim. Acta* **717**, 110–121 (2012). <https://doi.org/10.1016/j.aca.2011.12.046>
4. M.T. Ahmed, P.G. Clay, G.R. Hall, Radiation-induced decomposition of ion exchange resins: part II. The mechanism of the deamination of anion-exchange resins. *J. Chem. Soc. B* (1966). <https://doi.org/10.1039/j29660001155>
5. G.R. Hall, M. Streat, Radiation-induced decomposition of ion exchange resins: part I. Anion-exchange resins. *J. Chem. Soc.* **37**, 5205–5211 (1963). <https://doi.org/10.1039/jr9630005205>
6. L.L. Smith, H.J. Groh, The effect of Gamma radiation on ion exchange resins. Report DP-549: Department of Energy and Environment (1961). <https://doi.org/10.2172/4050930>
7. A. Traboulsi, V. Labeled, V. Dauvois et al., Gamma radiation effect on gas production in anion exchange resins. *Nucl. Instrum. Methods B* **312**, 7–14 (2013). <https://doi.org/10.1016/j.nimb.2013.06.021>
8. A. Baidak, J.A. Laverne, Radiation-induced decomposition of anion exchange resins. *J. Nucl. Mater.* **407**, 211–219 (2010). <https://doi.org/10.1016/j.jnucmat.2010.10.025>
9. L. Zhao, G. Yu, X.Y. Zhang et al., Diffusivity of hydrogen in steels at low temperatures. *Corros. Sci. Prot. Technol.* **17**, 349–351 (2005). <https://doi.org/10.3969/j.issn.1002-6495.2005.05.015>. (in Chinese)
10. X.L. Zhen, W.B. Kan, H.L. Pan, Study on hydrogen diffusion in 304 stainless steel. *Corros. Prot. Petrochem. Ind.* **27**, 15–16 (2010). <https://doi.org/10.3969/j.issn.1007-015X.2010.04.005>. (in Chinese)
11. T. Sullivan, Waste container and waste package performance modeling to support safety assessment of low and intermediate-level radioactive waste disposal. Technical Report BNL-74700-2005-IR: DOE/IAEA (US) (2004). <https://doi.org/10.2172/15016583>
12. H.Y. Jin, Estimating diffusion coefficients of gases by use of computer simulation. *Comput. Appl. Chem.* **29**, 1294–1298 (2012). <https://doi.org/10.3969/j.issn.1001-4160.2012.11.004>
13. C. Boher, F. Frizon, S. Lorente et al., Influence of the pore network on hydrogen diffusion through blended cement pastes. *Cem. Concr. Compos.* **37**, 30–36 (2013). <https://doi.org/10.1016/j.cemconcomp.2012.12.009>
14. H.T. Vu, F. Frizon, S. Lorente, Architecture for gas transport through cementitious materials. *J. Phys. D Appl. Phys.* **42**, 105501 (2009). <https://doi.org/10.1088/0022-3727/42/10/105501>
15. J. Sercombe, R. Vidal, C. Gallé et al., Experimental study of gas diffusion in cement paste. *Cem. Concr. Res.* **37**, 579–588 (2007). <https://doi.org/10.1016/j.cemconres.2006.12.003>
16. D.T. Niu, L.T. Chen, C.H. Zhang, Calculating model for gas diffusivity in concrete. *J. Xi'an Univ. Archit. Technol.* **39**(6), 741–745 (2007). <https://doi.org/10.3969/j.issn.1006-7930.2007.06.001>. (in Chinese)
17. Y.J. Tang, X.B. Zuo, G.J. Yin, Gas diffusion model in concrete based on pore structural parameters. *J. Build. Mater.* **18**, 976–981 (2015). <https://doi.org/10.3969/j.issn.1007-9629.2015.06.011>. (in Chinese)
18. F. Bardelli, C. Mondelli, M. Didier et al., Hydrogen uptake and diffusion in Callovo-Oxfordian clay rock for nuclear waste disposal technology. *Appl. Geochem.* **49**, 168–177 (2014). <https://doi.org/10.1016/j.apgeochem.2014.06.019>
19. C. Mondelli, F. Bardelli, J.G. Vitillo et al., Hydrogen adsorption and diffusion in synthetic Na-montmorillonites at high pressures and temperature. *Int. J. Hydrogen Energy* **40**(6), 2698–2709 (2015). <https://doi.org/10.1016/j.ijhydene.2014.12.038>
20. E. Jacobs, K. Wouters, G. Volckaert et al., Measuring the effective diffusion coefficient of dissolved hydrogen in saturated Boom Clay. *Appl. Geochem.* **61**, 175–184 (2015). <https://doi.org/10.1016/j.apgeochem.2015.05.022>